Coexistence of deep levels with optically active InAs quantum dots

S. W. Lin, C. Balocco, M. Missous, A. R. Peaker, and A. M. Song*
School of Electrical and Electronic Engineering, University of Manchester, Manchester M60 1QD, United Kingdom
(Received 2 June 2005; revised manuscript received 4 August 2005; published 3 October 2005)

We present direct experimental evidence of the coexistence of deep levels with intrinsic quantum confinement states in large, self-assembled InAs quantum dots embedded in a GaAs matrix. The InAs quantum dots show very good optical properties, as evidenced by the strong photoluminescence at room temperature at ~1.3 μm. Deep levels 160 and 484 meV below the GaAs conduction band edge have been identified at large reverse biases and high temperatures using deep level transient spectroscopy (DLTS) measurements. The reverse-bias dependence of the DLTS signal together with experimental results from the reference samples, containing thin InAs layers but no quantum dots, confirms that the deep levels coexist in the same layer as the InAs dots, and are most likely caused by the strain field during the lattice mismatched growth process. The densities of the deep levels in the structure are comparable to the density of the optically active quantum dots.

DOI: 10.1103/PhysRevB.72.165302 PACS number(s): 73.63.Kv, 73.20.Hb, 73.21.La, 73.61.Ey

Considerable efforts have been expended in the study of self-assembled semiconductor quantum dots (QDs), grown by the Stranski-Krastanov growth mode, because of their importance in device applications and in fundamental physics.[1,2] The excellent optical properties, such as strong photoluminescence (PL) intensity, are generally attributed to the coherent nature, i.e., defect free, of the QD islands.[1–6] In recent years, however, an increasing number of experiments have suggested the possibility that electronic deep levels might exist around or in what were regarded as coherent QDs that exhibit strong PL signals. For example, the presence of defects was suggested as a possible reason for the absence of the so-called phonon-bottleneck effect.[7,8] Other optical experiments, such as the quenching of PL signals at high temperatures, also suggested the possible existence of deep level defects around the QDs.[9–11] Dai *et al.* pointed out that the defect related centers existed at the InAs/GaAs interface and played an important role in the PL quenching process.[12] They also indicated that the energy of the interface defects depended on the size of the quantum dots. By performing time-resolved optical characterizations of InAs QDs in GaAs, Fiore *et al.* speculated on the existence of nonradiative traps in the (In)GaAs matrix in the close vicinity of the QDs, which would capture the carriers before they relaxed into the QDs.[13]

Despite the evidence of the existence of unknown deep levels, the optical experiments could not provide confirmation and direct information, such as energy levels and concentrations, of possible deep levels due to their generally nonradiative nature. The electrical space-charge technique, deep level transient spectroscopy (DLTS),[14] has recently been used to characterize QD structures, but most efforts have been focused on the intrinsic QD states.[15–21] The electrons can be thermally emitted out from the dots and then be detected by DLTS only when their electronic states are lifted above the bulk Fermi level. Therefore, by careful adjustment of the filling/reverse biases, electrons from the two intrinsic *s* states have been resolved successfully by this technique.[19–21] More importantly, the DLTS technique allows reliable determination of both the spatial and energy positions of nonradiative deep levels. Walther *et al.*[22] observed energy states approximately 400 meV below the GaAs conduction band edge in or near the quantum dots, and Wang *et al.*[6] and Krispin *et al.*[23] reported a series of defect states in their InAs/GaAs structures. Since no intrinsic quantum dot states were observed in these experiments, however, it was not clear whether these deep levels were actually present in optically active QD structures, and if so, whether they were spatially localized and whether they coexisted in the QD layers. Such information is important for physical studies and optimizations of both electronic and optical devices based on self-assembled QDs. It is also useful to determine if the deep levels result from the lattice mismatch induced strain, or the deep levels are actually created only during the Stranski-Krastanov island formation process.

In this work, we report on direct observation that deep levels coexist with the intrinsic quantum states of self-assembled InAs QDs using DLTS that exhibit strong PL intensity even at room temperature, at least for large, 1.3 μm emitting structures. This was possible by carrying out DLTS experiments at sufficiently high temperatures and large enough reverse biases. Bias-dependence experiments and calculations reveal that the deep levels are localized in space and indeed coexist in the QD layer. Investigations on the reference samples with only an InAs wetting layer but no QDs also show accumulation of the same types of deep levels, despite the absence of the QD states. This indicates that the deep levels are created by the lattice mismatch induced strain alone, rather than the Stranski-Krastanov QD formation process. The possible origin of the coexisting deep levels will be discussed.

Samples with either InAs QDs or only a pseudomorphic InAs wetting layer were studied in this work. The InAs layers (both QDs and pseudomorphic) were sandwiched by two 0.4-μm-thick Si-doped GaAs layers grown by molecular beam epitaxy (MBE) on (100) n^+-GaAs substrates as shown in Fig. 1(a). The growth was performed in an Oxford Instrument VGSemicon V90H system under the conditions that were tailored to yield large InAs QDs at a growth temperature of 480 °C. The GaAs matrix was grown at 580 °C. The formation of QDs with 2.8 ML coverage was monitored *in situ* by reflection high-energy electron diffraction (RHEED),

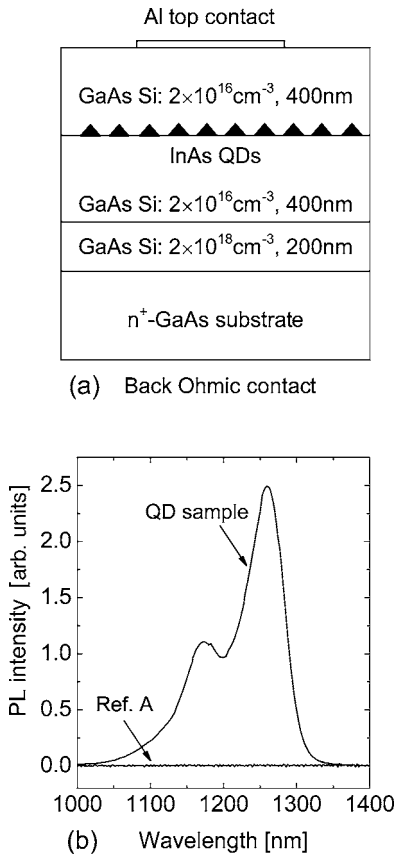

FIG. 1. (a) Schematics of the InAs QD material and device structures. (b) PL signals at room temperature for both the QD sample and reference sample A with a 1.2 ML InAs wetting layer.

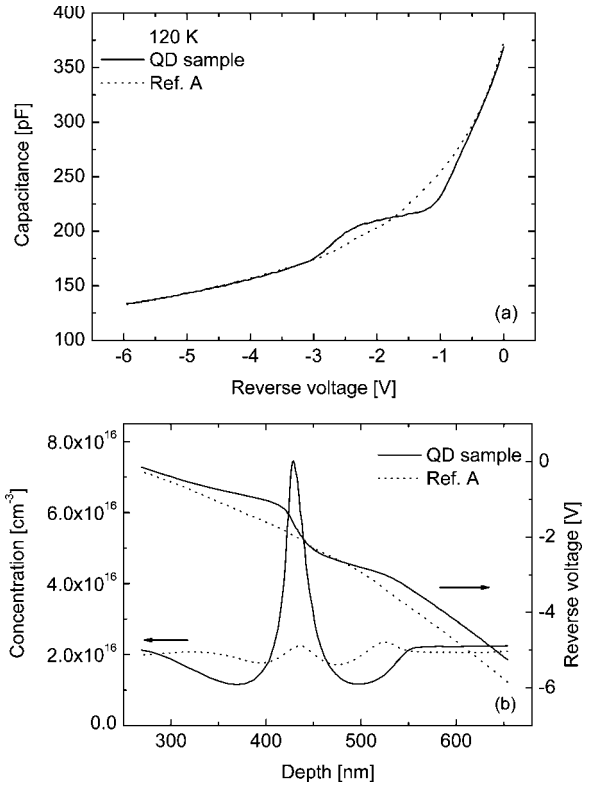

FIG. 2. (a) *C-V* characteristics and (b) the corresponding carrier concentration profiles taken at $T=120$ K and 1 MHz for both the QD sample and reference sample A with a 1.2 ML InAs wetting layer.

and the QD nucleation was observed via the change of the RHEED pattern from steady [two-dimensional (2D) growth] to spotty (3D growth). The resulting quantum dot density was around 3×10^9 cm^{-2}, as determined by imaging uncapped samples using an atomic force microscope (AFM), and is in the same order of magnitude as the density estimated from the DLTS signals. The ohmic contact was fabricated by alloying Au-Ge-Ni/Au on the back side of the structure and the top Schottky contacts, 1 mm in diameter, were defined by evaporating Al on the top surface.

PL measurements were performed at room temperature with laser excitation at a wavelength of 532 nm. The signal was dispersed by a monochromator and collected using an InGaAs detector for the wavelength range between 1000 and 1500 nm, while using a charge-coupled device (CCD) detector for shorter wavelengths. The large size of the dots correlates with a strong PL emission at about 1.26 μm shown in Fig. 1(b), which corresponds to the interband transition from the QD ground electronic state to the ground hole state.[24] In addition, the PL spectrum of the QD sample exhibits another peak at about 1.18 μm which is due to the recombination of ground-state electrons with holes in the first excited state.[24] The strong PL at room temperature shows that the QDs are optically active. This work examines whether such QDs would be defect free, that is, investigating if nonradiative deep levels exist in the QD layer.

For comparison, two reference samples with 1.2 and 1.5 ML InAs wetting layers (Referred to as Ref. A and Ref. B, respectively) were grown with exactly the same layer structures and under the same conditions as the QD sample. The PL signals from the GaAs matrix and InAs wetting layer in the reference samples are observed at around 890 and 910 nm, respectively, which are the same as those in the QD sample. The absence of QDs in the reference samples is confirmed by the disappearance of QD PL signals at room temperature as shown in Fig. 1(b). Since Ref. B shows very similar experimental results to Ref. A, in the following we concentrate on the results that have been obtained on the QD sample and Ref. A.

Figure 2(a) shows the capacitance-voltage (*C-V*) characteristics of the QD sample and reference sample A (Ref. A) measured at a temperature of $T=120$ K. The pronounced plateaulike structure of the QD sample occurring between the reverse biases $V_r=-3.0$ and -1.0 V, as compared with the almost smooth curve of the reference sample, suggests that certain electronic states exist in the QD layer that capture and emit electrons.[24,25] The capacitance value at the plateau agrees well with the distance between the QD layer and the Al top Schottky contact. The width of the plateau is determined by the energy spread of the electronic states.[19] Such states may be the intrinsic QD energy levels, deep levels due to defects, or both, and will be identified in the following DLTS experiments. The *C-V* result reveals that at $V_r=-1.0$ V the electronic states are lifted close to the bulk Fermi level, and electrons begin to escape from the states. At $V_r=-3.0$ V, all the electronic states involved are raised

above the Fermi level and are therefore fully discharged. The corresponding apparent carrier distributions of the QD and reference samples in Fig. 2(b) can be obtained from the local slope of the *C-V* curves,[26] and indicate electron accumulation in the QD/WL plane at around 400 nm under the Schottky contact, in good agreement with the location of the InAs layer from the growth parameters. There is another accumulation peak at around 530 nm in the Ref. A concentration profile, suggesting the electronic deep levels in the structure, which is confirmed by the DLTS data in the following. The charge on the deep levels can only be detected by applying sufficiently high reverse voltage at which the deep levels can be lifted above the bulk Fermi level. No similar peak is found in the electron concentration profile of the QD sample, probably because of the strong electrostatic field in the depletion regions on both sides of the pronounced QD accumulation peak and relatively lower densities of the deep levels in the QD structure.

To identify the nature of the electronic states that result in the plateau in the *C-V* characteristics, DLTS experiments were carried out in the QD and reference samples at different reverse biases. Five peaks are observed in the DLTS spectra of the QD sample as shown in Fig. 3(a), where the reverse bias V_r is between −2.5 and −5.0 V. The two peaks, marked as traps 1 and 2, can still be detected at much lower reverse biases $V_r > -1.5$ V (not shown here), when the intrinsic electron states in the QDs as well as any possible deep levels in the QD layer are well below the bulk Fermi energy. We therefore conclude that they are due to bulk electron traps. This is confirmed in other GaAs samples grown under the same condition but without an InAs layer. In the reference samples, these two traps are also observed despite their weaker densities. By comparison with the findings in the literature, we conclude that traps 1 and 2 are the M3 and E4 levels, respectively, which are commonly detected in GaAs materials grown by MBE.[27]

The pronounced peak at about 50 K at $V_r = -3.0$ V in Fig. 3(a) is attributed to the electron emission from the intrinsic states in the quantum dots since there is no such DLTS signature at a similar temperature in the DLTS spectra of the reference samples, shown in Fig. 3(b). The post-growth rapid thermal annealing (RTA) of the QD sample also confirms such an identification (detailed RTA results to be published elsewhere). We hence conclude that the pronounced plateau in the *C-V* trace in Fig. 2(a) is a result of capture and emission of electrons in the QDs in pace with the measurement frequency.

The activation energy of 76 meV, obtained from the Arrhenius plot in Fig. 4, is similar to the values reported by Kapteyn *et al.*[15,16] Using the same theory, we interpret the emission process as electrons in QDs being first thermally activated from the ground state into the excited states and then fast tunneling out from the excited states. The calculated thermal activation energy of 76 meV therefore corresponds to the energy difference between QD ground and excited states. As shown in Fig. 3(a) at different reverse biases, such QD thermal excited DLTS peaks are well resolved only at certain bias voltages. This is because when $V_r < -3.0$ V the emission is more dominated by tunneling, which is rather temperature independent and therefore less visible in the

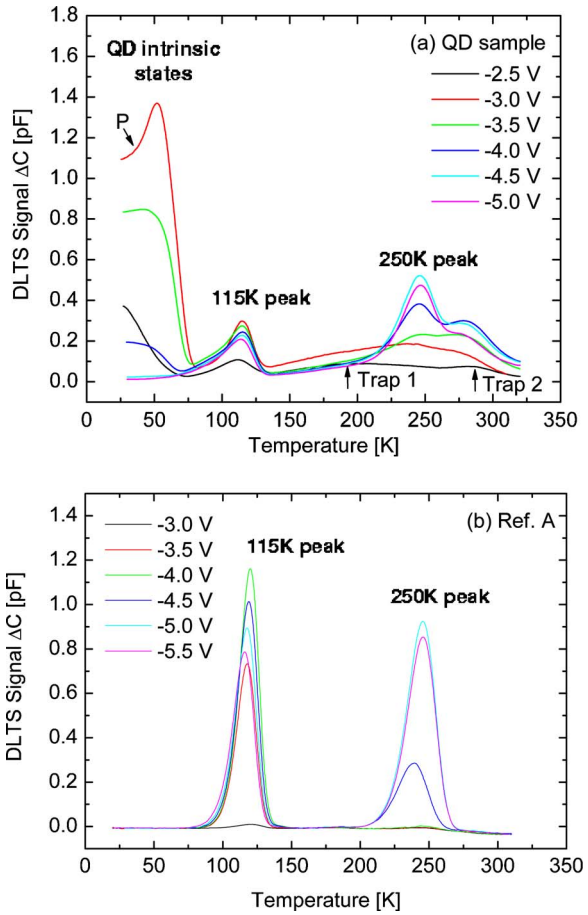

FIG. 3. (Color online) DLTS spectra for the QD sample (a) and Ref. A (b). The filling pulse bias is set to −0.5 V. The reverse bias is increased in steps of 0.5 V from −2.5 to −5.0 V and from −3.0 to −5.5 V for the QD sample and Ref. A, respectively. Referring to the DLTS peak positions, the two pronounced peaks observed in both samples are named as 115 K peak and 250 K peak, respectively. Traps 1 and 2 denote bulk defects in the QD sample. Arrow P in (a) shows the point at $T = 35$ K and $V_r = -3.0$ V where the tunneling rate directly from the QD ground state to GaAs conduction band is approximately equal to the thermal excitation rate from the ground state to the excited state.

DLTS spectra. The flat region in the DLTS spectrum at $V_r = -3.0$ V below 35 K is related to electron tunneling directly from the QD ground state into the GaAs conduction band. Assuming a triangular barrier, the tunneling rate can be written as

$$e_t = \frac{eF}{4\sqrt{2m^*\Delta E_t}} \exp\left(\frac{-4\sqrt{2m^*}\Delta E_t^{3/2}}{3e\hbar F}\right), \qquad (1)$$

where F is the electric field, e the electron charge, $\hbar$ the reduced Planck constant, m^* the GaAs effective electron mass, and ΔE_t the tunneling barrier height.[28,29] In order to estimate ΔE_t, we assume that the tunneling rate is approximately equal to the thermal excitation rate from the QD ground state to the excited state at $T = 35$ K, marked by the arrow P in Fig. 3(a). The obtained barrier height for the QD

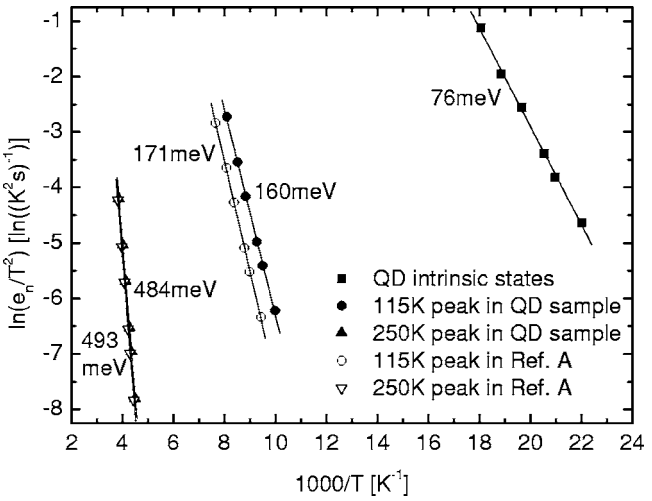

FIG. 4. Arrhenius plots of the emission rates determined from the maximum positions of the DLTS spectra at different rate windows. The activation energies are determined from the slopes of a linear fit to the data (straight lines). The apparent electron capture cross sections are determined from the intercepts of the linear fit on the vertical axes.

ground state is 171 meV, similar to the values reported by others.[15–21]

Apart from the QD signal in the DLTS spectra in Fig. 3(a), two pronounced peaks are located at about 115 and 250 K. In the DLTS spectra of Ref. A in Fig. 3(b), there are two DLTS peaks at similar temperature positions, suggesting that these 115 and 250 K peaks in the QD sample are not related to the QD intrinsic states but some deep levels in the structure. We can also conclude that these deep levels could be created by the strain field induced by the lattice mismatch alone, not necessarily due to the three-dimensional QD formation process.

From the Arrhenius plots in Fig. 4, the excitation energies of these two deep levels in the QD sample are determined to be about 160 and 484 meV, respectively. The bias dependence of the relative capacitance change, $\Delta C/\Delta C_{\max}$, shown in Fig. 5(a), indicates that the deep levels are not bulk defects, but have a rather narrow spatial distribution. Both peaks do not appear until the reverse biases reach their thresholds, at which their electronic energy states are raised up to the bulk Fermi energy. The 115 K peak starts to appear at $V_r=-2.0$ V and reaches its maximum at $V_r=-3.1$ V, whereas the 250 K peak starts at $V_r=-3.5$ V and becomes maximal at $V_r=-4.5$ V, as shown in Fig. 5(a). Beyond the maxima, the DLTS signals gradually decrease because the relative change in the capacitance becomes smaller due to the increased depletion depth. The behavior follows evidently from Eq. (2), which describes the relative DLTS peak amplitude for deep levels located on a plane[15,30]

$$\frac{\Delta C}{C}=\frac{n_T x_T}{w^2 N_d}. \tag{2}$$

Here, ΔC is the DLTS peak amplitude, C the steady state capacitance at the reverse bias, n_T the sheet density of the deep levels, x_T the distance between the top Schottky contact

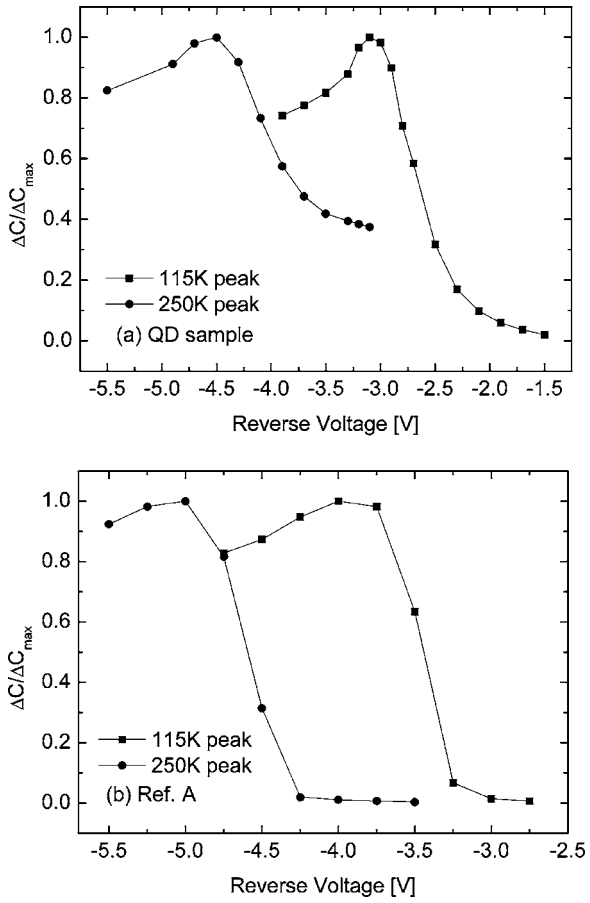

FIG. 5. Bias dependence of normalized DLTS peak height, $\Delta C/\Delta C_{\max}$, at 115 K (squares) and 250 K (dots) in the DLTS spectra of the QD sample (a) and Ref. A (b). The filling pulse bias is fixed at −0.5 V. Because of the presence of traps 1 and 2, the relative height of the 250 K peak can be determined reliably only when the bias is below −3.0 V in (a).

and the plane where the deep levels are located, w the depletion depth at the reverse bias, and N_d the doping concentration. Note that since the deep levels usually have a finite distribution of energy, n_T in Eq. (2) is a function of reverse bias. Below the threshold bias of the deep levels, n_T is equal to zero because all the electronic states are below the bulk Fermi level; when the reverse bias is larger than the threshold value, n_T increases with the increasing reverse bias, and then fixes at the maximal value when all the electronic states are raised above the Fermi level.

To determine the locations of the deep levels in the QD sample, we model the QD structure as an ideal Schottky diode and neglect the effect of charging and discharging of QDs on the electric field. By solving Poisson's equation, the potential profile of the QD structure is given by

$$V(x)=-\frac{eN_d}{2\varepsilon_0\varepsilon_r}(w-x)^2, \tag{3}$$

where ε_0 is the permittivity of free space, ε_r the GaAs dielectric constant, and x the distance from the top Schottky contact in the depletion region. Equation (2) shows that the

TABLE I. Data about the deep levels in the QD and reference samples, calculated from DLTS results.

	115 K peak			250 K peak		
	E_a (meV)[a]	σ (cm^2)[b]	Sheet density (cm^{-2})[c]	E_a (meV)	σ (cm^2)	Sheet density (cm^{-2})
QD sample	160	9.5×10^{-16}	2.5×10^{9}	484	1.9×10^{-13}	5.0×10^{9}
Ref. A	171	1.0×10^{-15}	1.1×10^{10}	493	2.1×10^{-13}	1.1×10^{10}
Ref. B	166	9.3×10^{-16}	1.4×10^{10}	495	2.4×10^{-13}	1.4×10^{10}

[a]Thermal excitation energy obtained from the slope of the Arrhenius plot.
[b]The apparent electron capture cross section taken from the intercept of the Arrhenius plot.
[c]Calculated from the maximal amplitude of the DLTS spectra by Eq. (1).

reverse bias to reach the maximal relative capacitance change, $\Delta C/\Delta C_{\max}$ in Fig. 5(a), neither exactly corresponds to the moment when the bulk Fermi level passes the full energy distribution of the deep levels, nor when the Fermi level aligns with the energy corresponding to the distribution peak. We therefore use the threshold biases, at which the deep levels start to be detected, to estimate their locations by applying Eq. (3). From the reverse bias threshold of the 115 K peak, $V_r=-2.0$ V, shown in Fig. 5(a), we obtain a location of 395 nm below the surface, in very good agreement with the designed QD location in the material (400 nm). From the threshold reverse bias of −3.5 V of the 250 K peak, the location is calculated to be about 391 nm below the surface, also well corresponding to the depth of the QD layer. Furthermore, when we etch off the capping layer and QD layer from the QD sample, we found no DLTS signals at around 50, 115, and 250 K, further supporting that the deep levels coexist in the dot layer. This is a direct observation and strong confirmation of the coexistence of deep levels with the intrinsic quantum dot states.

Experiments were also performed on the reference samples A and B. Both reference samples show very similar PL, DLTS spectra, and bias dependence of the relative capacitance change. Here we only show the results of Ref. A to compare with those of the QD sample. Figure 3(b) shows no QD DLTS peak at around 50 K in Ref. A, in agreement with the room temperature PL in Fig. 1(b). This is as expected since the InAs layer is well below the critical thickness of 1.7 ML for QD formation. However, two strong DLTS peaks appear at about 115 and 250 K, the same positions as those of the deep levels in the QD sample, shown in Fig. 3(a). The Arrhenius plots shown in Fig. 4 allow us to calculate their thermal activation energies and the corresponding apparent electron capture cross sections, which are listed in Table I for comparison with the results in the QD sample. For both the 115 and 250 K peaks, the activation energies and capture cross sections in the reference samples are quite close to those in the QD sample. In addition, as shown in Figs. 5(a) and 5(b), the bias dependences of the DLTS spectra in the QD and Ref. A samples are very similar, with virtually the same threshold biases. This also confirms that they are spacially localized in the growth direction.

A close look at Fig. 5 reveals a difference in the threshold biases of the peaks between the QD and reference samples. This is expected because of the unintentional fluctuations in the doping concentrations in the two materials, the different surface Fermi level pinning caused by slight variations in the sample fabrications, etc. By determining the threshold biases and applying the same calculation model as above, the 115 and 250 K peaks in the reference samples have almost identical locations, also confirming that these two types of deep levels coexist in the same layer. Furthermore, the calculated depth is very close to the growth parameter. All the evidence above from the QD sample and the two reference samples thus suggests that the deep levels related to the 115 K peak among the three samples are the same type of defects, and so are the deep levels related to the 250 K peak in the three samples.

We now discuss the origins of such coexisted deep levels in the InAs layer. Two categories of defects are usually observed in semiconductors: one is extended defects such as dislocations, and the other is point defects, such as vacancies, interstitials, or chemical impurities in the lattice. The analysis of our experimental results below rules out the possibility of being dislocation related extended defects. Instead, the observed deep levels might be some type of point defects introduced by the lattice mismatch strain during the growth process.

The previous work by Wang *et al.* on the relaxation-induced defects in QD structures indicated that beyond the critical coverage of about three monolayers of InAs, threading dislocations and stacking faults could appear in the GaAs cap layer, whereas misfit dislocation and cross-hatched stacking faults might appear near the QDs boundary.[6] In comparison with the experimental results by Wang *et al.*, the coexisted deep levels in our samples have different activation energies and apparent electron capture cross sections. Furthermore, the thickness of our InAs QD layer is 2.8 ML, less than the reported critical thickness of three monolayers. More importantly, we observe strong photoluminescence signals even at room temperature and apparent quantum confinement in the *C-V* and DLTS measurements. We therefore conclude that the deep levels observed in our experiments are not dislocation-related traps.

M-series defects, reported by Lang,[31] are commonly observed bulk defects in MBE-grown GaAs, which are attributed to defect-impurity complexes with growth temperature dependent concentrations. M1 and M4 have similar DLTS signatures and thermal activation energies to the observed deep levels in our QD and reference samples. However, the concentrations of M1 and M4 are typically very low, around 10^{12} cm^{-3} at a growth temperature of 580 °C.[27] In order to compare the densities of the deep levels with those bulk defects commonly presented in MBE-grown GaAs, the volume

densities of deep levels in our samples can be simply calculated from

$$N_v = 2(\Delta C/C)N_d, \tag{4}$$

a formula used to evaluate the densities of bulk defects in GaAs.[14] The densities of the deep levels related to the 115 and 250 K peaks are thus calculated to be 5.7×10^{13} and 1.3×10^{14} cm^{-3}, respectively, in the QD sample, and 2.8×10^{14} and 3.2×10^{14} cm^{-3}, respectively, in the Ref. A sample. The densities are therefore more than one order of magnitude higher than those of M1 and M4 in MBE-grown GaAs under the similar growth conditions. Furthermore, the observed deep levels in our samples are localized in space and coexist in the InAs layer. There hence is a possibility that the strain field, induced by the lattice mismatch between the InAs and GaAs, could enhance the creation of M1 and M4, and localize them by inducing migration of M1 and M4 from neighboring layers. Since the strain around the dots is quite different from that between the dots, the DLTS peak shapes of the deep levels in the QD sample should be different from the symmetric DLTS signature of the ideal bulk defects, which might be reflected by the observation that the 115 and 250 K peaks in our QD sample are broadened and extended on the low temperature sides.

Another possibility is that the coexisted deep levels are native point defects caused by the strain during the InAs/GaAs growth process. From the DLTS amplitudes, the sheet densities of these deep levels can be calculated (see Table I), and are found to be comparable with the QD density determined by AFM scans. Note that in both reference samples the sheet density ratio between the 115 and 250 K deep levels is 1:1, strongly suggesting that these two deep levels have the same origin. The lattice mismatch between InAs and GaAs is 7.2%. The strain is built up by growing InAs on GaAs, until the growth mode changes from 2D to 3D and QDs form to relax the strain. The point defects related to 115 and 250 K DLTS peaks, such as vacancies and interstitials, might be introduced by the strain during the growth process and accumulated in the pseudomorphic wetting layer in the reference samples. As shown in Table I, the sheet densities of the deep levels in Ref. B are larger than those in Ref. A, which could be because the strain field in Ref. B with a 1.5 ML InAs layer is much stronger than in Ref. A with a 1.2 ML InAs layer. In the QD sample, much of the strain is relaxed by the formation of QDs, which can explain the lower sheet densities of the deep levels. The partial strain relaxation in the QD sample may also cause a broadening in the energy distribution of the deep levels, which may be the reason for the wider DLTS peaks shown in Fig. 3(a). Interestingly, the sheet density ratio between the 115 and 250 K deep levels is 1:2, rather than 1:1 in the reference samples. The reason is unknown and is subject to future studies.

Moreover, although the formation of QDs relaxes some of the strain, the remaining strain still exists in and around QDs. It has also been shown that strain field can extend from the QDs into surrounding GaAs matrix over a typical scale of $\geqslant$10 nm.[32–34] The extended strain field might cause migrations of native defects, such as vacancies and interstitials, to the vicinity of the quantum dots. During our sample growth, because of the relatively thick upper GaAs confining layers, the dots were subjected to an anneal of about 20 min at 580 °C, which could enhance the migration of the defects. Such accumulation of defects is in agreement with the previous observation by Walther *et al.*, where the clustering of the trap states occurred in regions of randomly higher quantum dot concentration.[22]

Having identified the deep levels coexisting in the same layer of QDs and their sheet densities, it is important to gain further insight into the effect of the deep levels on the properties of the QD structure, which may allow improvements of the optical and electrical properties of the QD materials. Sercel proposed that the presence of interface states or point defects formed during the growth process and correlated with the QDs could provide an efficient relaxation path for electrons through multiphonon-assisted tunneling.[8] Such lack of phonon bottleneck effect was found in recent time-resolved PL measurements, which was in disagreement with the theoretical prediction for an ideal quantum dot.[35,36] The binding energy of the QD ground state in our QD sample has been estimated to be 171 meV, close to the 160 meV of the coexisted deep level related to the 115 K DLTS peak. If the deep states lie close to the QDs, they may strongly couple with the dots and provide a rapid energy-relaxation channel through which electrons thermalize to enhance the luminescence efficiency.[8] For electronic device applications, the existence of states that are much deeper than the intrinsic QD states could be utilized to design memory devices. We recently demonstrated a fully electrically controlled, room temperature memory device where InAs QDs were embedded in a modulation-doped high electron-mobility transistor structure. The coexistence of similar deep levels in the QD layer was confirmed by the experiments using different gate biases to control the transfer of electrons between the deep levels and a two-dimensional electron gas.[37] In such devices, the slow charging of the deep levels, rather than the emission or discharging process, provided a long memory time even at room temperature.

In summary, we have presented the direct observation of the coexistence of deep levels in the same layer of optically active QDs. The deep levels are found to be caused by the strain rather than the formation of 3D QDs. Further studies of such deep levels by DLTS together with optical characterizations under different growth conditions could lead to important implications in optimization of the performance of QD-based electronic and optical devices.

The authors would like to thank V. P. Markevich and I. D. Hawkins for valuable discussions and technical support and M. Kaniewska for sending us a preprint of her work on deep states in InAs/GaAs. This work was supported by the Engineering and Physical Science Research Council (EPSRC) GR/S17741/01 and EP/C009738/1, and by Oxford Instrument Plasma Technology.

*Corresponding author. Email address: A.Song@manchester.ac.uk

[1] D. Bimberg, M. Grundmann, and N. N. Ledentsov, *Quantum Dot Heterostructures* (Wiley, Chichester, 1998).
[2] P. M. Petroff, A. Lorke, and A. Imamoglu, Phys. Today **54**, 46 (2001).
[3] Q. Xie, A. Madhukar, P. Chen, and N. P. Kobayashi, Phys. Rev. Lett. **75**, 2542 (1995).
[4] M. Grundmann, J. Christen, N. N. Ledentsov, J. Bohrer, D. Bimberg, S. S. Ruvimov, P. Werner, U. Richter, U. Gosele, J. Heydenreich, V. M. Ustinov, A. Y. Egorov, A. E. Zhukov, P. S. Kop'ev, and Z. I. Alferov, Phys. Rev. Lett. **74**, 4043 (1995).
[5] R. Heitz, T. R. Ramachandran, A. Kalburge, Q. Xie, I. Mukhametzhanov, P. Chen, and A. Madhukar, Phys. Rev. Lett. **78**, 4071 (1997).
[6] J. S. Wang, J. F. Chen, J. L. Huang, P. Y. Wang, and X. J. Guo, Appl. Phys. Lett. **77**, 3027 (2000).
[7] A. D. Yoffe, Adv. Phys. **50**, 1 (2001).
[8] P. C. Sercel, Phys. Rev. B **51**, 14532 (1995).
[9] J. Bloch, J. Shah, L. N. Pfeiffer, K. W. West, and S. N. G. Chu, Appl. Phys. Lett. **77**, 2545 (2000).
[10] Kohki Mukai, Nobuyuki Ohtsuka, and Mitsuru Sugawara, Appl. Phys. Lett. **70**, 2416 (1997).
[11] E. C. Le Ru, P. D. Siverns, and R. Murray, Appl. Phys. Lett. **77**, 2446 (2000).
[12] Y. T. Dai, J. C. Fan, Y. F. Chen, R. M. Lin, S. C. Lee, and H. H. Lin, J. Appl. Phys. **82**, 4489 (1997).
[13] A. Fiore, P. Borri, W. Langbein, J. M. Hvam, U. Oesterle, R. Houdré, R. P. Stanley, and M. Ilegems, Appl. Phys. Lett. **76**, 3430 (2000).
[14] D. V. Lang, J. Appl. Phys. **45**, 3023 (1974).
[15] C. M. A. Kapteyn, F. Heinrichsdorff, O. Stier, R. Heitz, M. Grundmann, N. D. Zakharov, D. Bimberg, and P. Werner, Phys. Rev. B **60**, 14265 (1999).
[16] C. M. A. Kapteyn, M. Lion, R. Heitz, D. Bimberg, P. N. Brunkov, B. V. Volovik, S. G. Konnikov, A. R. Kovsh, and V. M. Ustinov, Appl. Phys. Lett. **76**, 1573 (2000).
[17] H. L. Wang, F. H. Yang, S. L. Feng, H. J. Zhu, D. Ning, H. Wang, and X. D. Wang, Phys. Rev. B **61**, 5530 (2000).
[18] S. Ghosh, B. Kochman, J. Singh, and P. Bhattacharya, Appl. Phys. Lett. **76**, 2571 (2000).
[19] O. Engström, M. Malmkvist, Y. Fu, H. Ö. Olafsson, and E. Ö. Sveinbjörnsson, Appl. Phys. Lett. **83**, 3578 (2003).
[20] O. Engström, M. Kaniewska, Y. Fu, J. Piscator, and M. Malmkvist, Appl. Phys. Lett. **85**, 2908 (2004).
[21] S. Schulz, S. Schnull, C. Heyn, and W. Hansen, Phys. Rev. B **69**, 195317 (2004).
[22] C. Walther, J. Bollmann, H. Kissel, H. Kirmse, W. Neumann, and W. T. Masselink, Appl. Phys. Lett. **76**, 2916 (2000).
[23] P. Krispin, J.-L. Lazzari, and H. Kostial, J. Appl. Phys. **84**, 6135 (1998).
[24] P. N. Brounkov, A. Polimeni, S. T. Stoddart, M. Henini, L. Eaves, P. C. Main, A. R. Kovsh, Yu. G. Musikhin, and S. G. Konnikov, Appl. Phys. Lett. **73**, 1092 (1998).
[25] R. J. Luyken, A. Lorke, A. O. Govorov, J. P. Kotthaus, G. Medeiros-Ribeiro, and P. M. Petroff, Appl. Phys. Lett. **74**, 2486 (1999).
[26] P. Blood and J. W. Orton, *The Electrical Characterization of Semiconductors: Majority Carriers and Electron States* (Academic Press, London, 1992).
[27] P. Blood and J. J. Harris, J. Appl. Phys. **56**, 993 (1984).
[28] E. N. Korol, Sov. Phys. Solid State **14**, 1327 (1977).
[29] G. Vincent, A. Chantre, and D. Bios, J. Appl. Phys. **50**, 5484 (1979).
[30] M. Geller, C. Kapteyn, E. Stock, L. Müller-Kirsch, R. Heitz, and D. Bimberg, Physica E (Amsterdam) **21**, 474 (2004).
[31] D. V. Lang, A. Y. Cho, A. C. Gossard, M. Ilegems, and W. Wiegmann, J. Appl. Phys. **47**, 2558 (1976).
[32] M. Grundmann, O. Stier, and D. Bimberg, Phys. Rev. B **52**, 11969 (1995).
[33] D. Leonard, M. Krishnamurthy, C. M. Reaves, S. P. Denbaars, and P. M. Petroff, Appl. Phys. Lett. **63**, 3203 (1993).
[34] L. J. M. Selen, L. J. van IJzendoorn, M. J. A. deVoigt, and P. M. Koenraad, Phys. Rev. B **61**, 8270 (2000).
[35] U. Bockelmann and G. Bastard, Phys. Rev. B **42**, 8947 (1990).
[36] H. Benisty, C. M. Sotomayor-Torres, and C. Weisbuch, Phys. Rev. B **44**, R10945 (1991).
[37] C. Balocco, A. M. Song, and M. Missous, Appl. Phys. Lett. **85**, 5911 (2004).